MOLECULAR ECOLOGY

Molecular Ecology (2016) **25**, 104–120 doi: 10.1111/mec.13476

DETECTING SELECTION IN NATURAL POPULATIONS: MAKING SENSE OF GENOME SCANS AND TOWARDS ALTERNATIVE SOLUTIONS

Detecting spatial genetic signatures of local adaptation in heterogeneous landscapes

BRENNA R. FORESTER,* MATTHEW R. JONES,† STÉPHANE JOOST,‡ ERIN L. LANDGUTH† and JESSE R. LASKY§¶

*Nicholas School of the Environment, University Program in Ecology, Duke University, Durham, NC 27708, USA, †Division of Biological Sciences, University of Montana, Missoula, MT 59812, USA, ‡Ecole Polytechnique Fédérale de Lausanne (EPFL), School of Architecture, Civil and Environmental Engineering (ENAC), Laboratory of Geographic Information Systems (LASIG), CH-1015 Lausanne, Switzerland, §Earth Institute, and Department of Ecology, Evolution & Environmental Biology, Columbia University, New York, NY 10027, USA, ¶Department of Biology, Pennsylvania State University, University Park, PA 16802, USA

Abstract

The spatial structure of the environment (e.g. the configuration of habitat patches) may play an important role in determining the strength of local adaptation. However, previous studies of habitat heterogeneity and local adaptation have largely been limited to simple landscapes, which poorly represent the multiscale habitat structure common in nature. Here, we use simulations to pursue two goals: (i) we explore how landscape heterogeneity, dispersal ability and selection affect the strength of local adaptation, and (ii) we evaluate the performance of several genotype–environment association (GEA) methods for detecting loci involved in local adaptation. We found that the strength of local adaptation increased in spatially aggregated selection regimes, but remained strong in patchy landscapes when selection was moderate to strong. Weak selection resulted in weak local adaptation that was relatively unaffected by landscape heterogeneity. In general, the power of detection methods closely reflected levels of local adaptation. False-positive rates (FPRs), however, showed distinct differences across GEA methods based on levels of population structure. The univariate GEA approach had high FPRs (up to 55%) under limited dispersal scenarios, due to strong isolation by distance. By contrast, multivariate, ordination-based methods had uniformly low FPRs (0–2%), suggesting these approaches can effectively control for population structure. Specifically, constrained ordinations had the best balance of high detection and low FPRs and will be a useful addition to the GEA toolkit. Our results provide both theoretical and practical insights into the conditions that shape local adaptation and how these conditions impact our ability to detect selection.

Keywords: CDPOP, complex landscapes, genome scans, latent factor mixed model, natural selection, ordination methods

Received 20 June 2015; revision received 10 November 2015; accepted 10 November 2015

Introduction

Understanding the role of the environment in driving spatial patterns of biodiversity is a central goal in evolutionary biology and ecology. Local adaptation to environmental conditions is a major source of such spatial patterns. The extent of local adaptation is largely shaped by the interaction between selection and gene flow along selective gradients (Haldane 1930; Mayr 1963; Slatkin 1973; Nagylaki 1975; Felsenstein 1976; García-Ramos & Kirkpatrick 1997; Lenormand 2002). When selection is weak relative to gene flow, local adaptation may be inhibited due to migration load (Lenormand 2002). Conversely, when selection is strong local adaptation may occur under a migration–selection

Correspondence: Brenna R. Forester, Fax: (919) 684 8741; E-mail: brenna.forester@duke.edu

balance due to selection against maladapted migrants (Yeaman & Whitlock 2011). However, at low levels of dispersal when genetic variance within populations limits adaptation, increasing dispersal may increase genetic variance and favour local adaptation (Barton 2001; Bell & Gonzalez 2011). Many theoretical approaches to studying spatial patterns of biodiversity have tended to be in systems that are spatially implicit or have a one-dimensional linear environmental gradient (e.g. Holt & Gaines 1992; Kirkpatrick & Barton 1997; Mouquet & Loreau 2003). However, the geometry, or spatial structure, of environmental gradients may play an important role in determining spatial patterns of biodiversity (Felsenstein 1977; Palmer 1992; Lenormand 2002; Holt & Barfield 2011; Frean *et al.* 2013; Schiffers *et al.* 2014).

The spatial configuration of the landscape (i.e. arrangement of, and distance between habitat patches) can affect the probability of gene flow between habitats and therefore have important implications for the generation and maintenance of local adaptation (reviewed in Hedrick 1986, 2006; Lenormand 2002; Kawecki & Ebert 2004). For a given strength of selection gradient, local adaptation may be facilitated in landscapes with a high level of habitat aggregation (e.g. shallow continuous environmental gradients, Fig. 1a, and large homogenous habitat patches, Fig. 1c,d) because migrants will often disperse into similar environments (Endler 1973; Slatkin 1973). By contrast, in landscapes with low levels of habitat aggregation (e.g. highly heterogeneous habitats, Fig. 1b), local adaptation may be weaker as gene flow between these habitats overwhelms selection (Garant *et al.* 2007). Importantly, these outcomes largely depend on the interaction of habitat configuration with levels of dispersal and selection strength (Slatkin 1973; Garant *et al.* 2007). For example, empirical studies have demonstrated patterns of fine-scale local adaptation (i.e. microgeographic adaptation) to heterogeneous habitats when dispersal is low (Tack & Roslin 2010; Paccard *et al.* 2013). To provide insight into the expected frequency and strength of local adaptation in nature, we must characterize how habitat heterogeneity, dispersal and selection interact (Richardson *et al.* 2014). However, there have been few studies conducted on heterogeneous landscapes with a multi-scale structure approaching the spatial continuum common in nature (Schiffers *et al.* 2014). Studying the

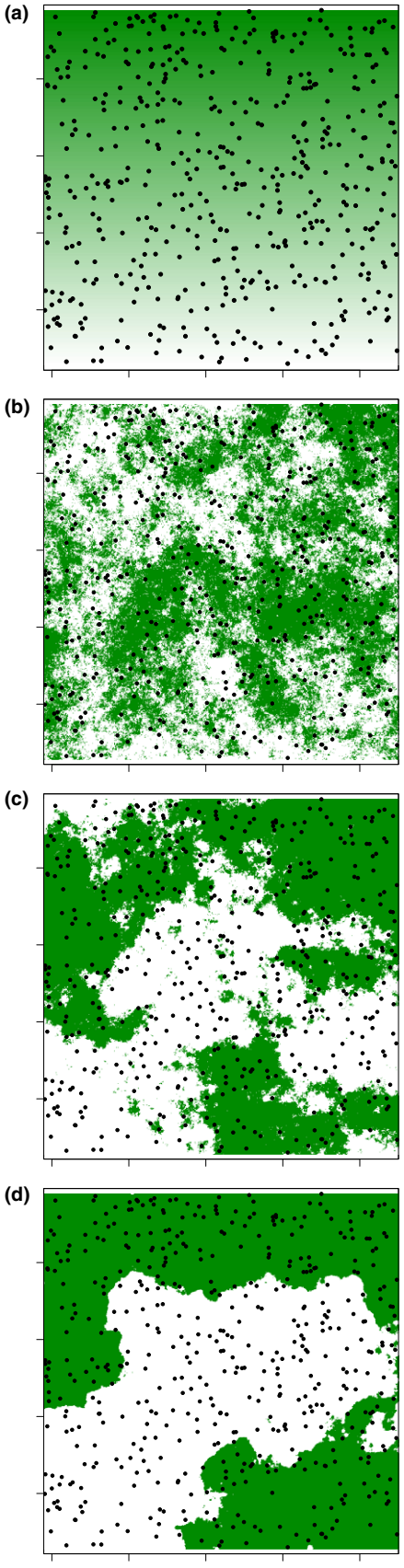

Fig. 1 Landscape selection configurations used for simulations. (a) Continuous selection gradient representing selection for *AA* genotypes in the north (dark) and *aa* genotypes in the south (light). Examples of discrete selection landscapes, from least to most aggregated: (b) H1, (c) H5 and (d) H9. Dark areas represent *AA* habitat and light areas represent *aa* habitat. Points represent the 500 sampled individuals.

effects of migration, selection and spatial structure is essential in realistic landscapes given that increasing complexity in the spatial structure of environments may generate counter-intuitive effects on local adaptation (Holt & Barfield 2011).

One approach to characterizing empirical patterns of local adaptation is to examine the extent to which spatial environmental variation coincides with genotypic variants (Hedrick *et al.* 1976; Mitton *et al.* 1977), i.e. genotype–environment association (GEA) methods (e.g. Joost *et al.* 2007, 2013; Coop *et al.* 2010; Frichot *et al.* 2013; Rellstab *et al.* 2015). GEA methods can be used to detect selection in cases where environmental gradients are continuous and when populations are not clearly distinguishable (Jones *et al.* 2013). This is an advantage when studying species that do not group into discrete populations or habitat types, or when studying species for which there is little prior ecological or genetic information (Jones *et al.* 2013; Joost *et al.* 2013). Simulation studies have examined the ability of GEA methods to detect selection under different scenarios of selection intensity, population structure and sampling schemes (De Mita *et al.* 2013; Jones *et al.* 2013; De Villemereuil *et al.* 2014; Lotterhos & Whitlock 2015). However, to date, few simulation studies have addressed the effect of spatially heterogeneous selection surfaces on the performance of GEA methods. Additionally, no simulation studies have addressed how the interactions between landscape heterogeneity, dispersal and selection affect our ability to detect local adaptation using GEA approaches.

Here, we explore the effects of environmental heterogeneity, dispersal ability and selection on the strength of local adaptation through simulations. A simulation framework is valuable because it allows for stochastic demography and evolution, and also makes the study of complex landscapes more tractable compared with analytical models (Bridle *et al.* 2010). We test a suite of GEA methods in the simulation parameter space to determine how these factors impact our ability to detect patterns of local adaptation. A major difficulty in any approach to detect selection in the genome is distinguishing between patterns of selection and population history or structure (e.g. population expansions, population bottlenecks, isolation by distance). Patterns resulting from population history can generate genotype–environment correlations similar to those underlying local adaptation, resulting in high false-positive rates (i.e. incorrectly identifying a locus as under selection when it is not, Jensen *et al.* 2005; Meirmans 2012). One way to overcome this problem is to control for genomewide patterns of variation, assumed to reflect population history. Several univariate mixed-model-based GEA approaches have been used to limit false positives (e.g. generalized linear and additive mixed models, Jones *et al.* 2013; models using an empirical covariance matrix, Günther & Coop 2013; and latent factor mixed models, LFMM, Frichot *et al.* 2013). However, univariate approaches, which test one locus and one predictor variable at a time, are not ideal because in reality, selection affects many loci and is driven by many variables simultaneously (Hahn 2008; Orsini *et al.* 2012). Some multivariate methods, which take high-dimensional multilocus genetic data and reduce it into a lower dimensional space, may be able to account for the joint action of selection and demography across the genome. For instance, ordination methods, which have a long history in plant and community ecology (Whittaker 1967; Van den Wollenberg 1977; Austin 1987; ter Braak 1987; Fitzpatrick & Keller 2015), extract trends from multivariate data by summarizing these data into a reduced set of uncorrelated axes (Jombart *et al.* 2009; Legendre & Legendre 2012). The similarities between community ecology and genomic data, namely a large number of variables (species or loci) observed at a set of sampling locations (sites or individuals/demes), imply that these analytical techniques could be effectively applied to large genomic data sets (e.g. Fitzpatrick & Keller 2015).

In a GEA framework, we can potentially distinguish outliers by looking for loci that show unique or unusual patterns in the ordination space. Because the ordination is explaining covariation in the data, we expect it to model patterns that affect the majority of the loci, such as those that arise due to population history. While principal components analysis, a common ordination technique, has been used to detect population structure in genetic data for nearly 50 years (Cavalli-Sforza 1966), only recently has it been used to correct for population structure in genomewide association studies (akin to GEA, Price *et al.* 2006; Patterson *et al.* 2006). In a novel use of ordination for multivariate outlier detection, Lasky *et al.* (2012) used redundancy analysis to quantify SNP variation in georeferenced *Arabidopsis* accessions with reference to geography and climate variables. We build on this and other recent empirical work using ordination methods for outlier detection (Duforet-Frebourg *et al.* 2015; Galinsky *et al.* 2015) by assessing a suite of ordination methods and a computationally efficient correlative mixed-model approach for their ability to detect selected loci under various spatial selection regimes.

Materials and methods

Simulation framework

We conducted simulations in the program CDPOP v1.2 (Landguth & Cushman 2010), which models population

genetic change across a landscape surface as a function of mutation, mating, gene flow, drift and selection. Our simulations consisted of 5000 diploid individuals with 100 bi-allelic loci; one of these loci was subject to selection (except for 'no selection' runs; see details below). All loci experienced a 0.0005 mutation rate per generation, free recombination and no physical linkage. We ran 10 Monte Carlo replicates of each simulation for a total of 1250 generations, discarding the first 250 generations as burn-in (no selection imposed) to establish a spatial genetic pattern prior to initiating the landscape selection configurations. Three of the simulations were run with a zero mutation rate to assess the impact of mutation rate on detection results (Table S1, Supporting information).

Simulation scenarios

We generated simulations under different combinations of landscape selection configuration, selection strength and dispersal capacity. We tested two types of landscape selection configurations: a continuous selection gradient landscape and discrete selection landscapes (Fig. 1). In the continuous selection gradient landscape (referred to as 'G' landscapes), selection acted in a continuous clinal fashion along an environmental gradient with different homozygous genotypes (*AA* and *aa*) favoured at different ends of the gradient (referred to as north and south), reflecting a pattern of antagonistic pleiotropy (Fig. 1a; Jones *et al*. 2013). Discrete selection landscapes included discrete habitat types (type '*AA*' or '*aa*', Fig. 1b–d) in which *AA* and *aa* genotypes were favoured in their respective habitat patches. For the discrete selection scenarios, we used the neutral landscape model QRULE (Gardner 1999) to simulate binary landscape maps (1024 × 1024 pixels). Habitat fragmentation was controlled with the *H* parameter, which affects the aggregation of habitat pixels; higher values of *H* lead to higher levels of aggregation. The discrete landscapes consisted of 50% of each habitat type and aggregation levels of $H = 0.1$ ('H1', Fig. 1b), 0.5 ('H5', Fig. 1c) and 0.9 ('H9', Fig. 1d). We produced 10 replicate landscapes for each *H* value to average across stochastic variation among simulated landscapes.

Across these different spatial selection configurations, we tested the effects of varying selection strength, mediated through density-independent (i.e. environment-driven) mortality (*s*) determined by genotypes at the selected locus. Selection strengths included $s = 0.01$ or '1%', $s = 0.05$ or '5%', $s = 0.10$ or '10%', and $s = 0.50$ or '50%'. We also included simulations with 'no' selection ($s = 0$) as a null model. In the continuous selection gradient scenario, *AA* experienced 0% mortality in the north and *s* mortality (either 1%, 5%, 10% or 50%) in the south, while the *aa* genotype was given the opposite selection gradient surface (0% mortality in the south and *s* mortality in the north). The *Aa* genotype experienced uniform density-independent mortality across the surface equal to the mean mortality of the two homozygotes at the extreme ends of the gradient ($s/2$; e.g. 25% density-independent mortality for 50% selection). For the discrete selection landscape scenarios, *AA* individuals had no mortality in '*AA*' patches and experienced 1%, 5%, 10% or 50% mortality if they occurred in '*aa*' patches. Individuals with *aa* genotypes at the locus under selection experienced the opposite selection gradient. The *Aa* genotypes again experienced uniform selection ($s/2$) across the entire surface.

Finally, we tested the effects of six dispersal levels (3%, 5%, 10%, 15%, 25% and 50%) that represent the maximum percentage of the landscape surrounding an individual that is available for movement and mating. These dispersal levels represent a range of biologically realistic dispersal distances per generation, from minimal dispersal (3%, e.g. terrestrial salamanders or gravity-dispersed seeds) to long-distance dispersal (50%, e.g. passerine birds or wind-dispersed seeds). Mating pairs of individuals and dispersal locations of offspring were chosen based on a random draw from the inverse-square probability function of distance, truncated with the specified maximum distance.

Mating parameters represented a population of unisexual individuals with females and males mating with replacement. The number of offspring produced from mating was determined from a Poisson distribution ($\lambda = 4$), which produced an excess of individuals each generation to maintain a constant population size of 5000 individuals at every generation. Carrying capacity of the simulation surface was 5000 individuals. Excess individuals were discarded once all 5000 locations became occupied, which is equivalent to forcing out emigrants once all available home ranges are occupied (Balloux 2001; Landguth & Cushman 2010).

Isolation by distance and local adaptation

We sampled 500 randomly selected individuals from the 5000 available individuals in the simulation space. This same set of 500 individuals was sampled from each simulation for all subsequent analyses (plotted in Fig. 1). We did not vary sample size or sampling scheme in this analysis, although assessing the impact of sample size and sampling approaches will be an important area for follow-up (see 'Future directions'). We measured isolation by distance (IBD) across all loci in each simulation using spatial eigenfunction analysis and multivariate linear regression, as

proposed by Diniz-Filho *et al.* (2013) and Legendre *et al.* (2015). First, we applied a principal coordinate analysis (PCoA, details below) to the pairwise multivariate genetic distance matrix, which was calculated using Bray–Curtis distance (Bray & Curtis 1957). We retained PCoA axes based on the broken-stick criterion (Legendre & Legendre 2012); retained axes were used as the response data in the subsequent redundancy analysis (multivariate linear regression, or RDA, details below). Spatial eigenfunctions (distance-based Moran's eigenvector maps, dbMEMs) were calculated from the coordinates of the samples and used as predictors in the RDA. Forward selection was used to reduce the number of dbMEMs (Blanchet *et al.* 2008). We calculated adjusted R^2 statistics (R^2_{adj}) and assessed significance using 1000 permutations. These analyses used the packages 'VEGAN' (Oksanen *et al.* 2013), 'PCNM' (Legendre *et al.* 2012), 'BOOT' (Canty & Ripley 2012) and 'PACKFOR' (Dray *et al.* 2011) in R v. 2.15.2 (R Development Core Team 2012). These results were compared to r^2 values derived from simple Mantel's tests of Bray–Curtis genetic distances and the log of geographic distance, using the 'ECODIST' package (Goslee & Urban 2007). Mantel r values were squared to facilitate comparison with R^2_{adj} statistics from spatial eigenfunction and redundancy analysis (Table S2, Supporting information).

To assess the strength of local adaptation, we quantified the relationship between allele frequencies and selection gradients. To do so, we converted the allele frequency at the locus under selection to the number of '*A*' alleles, and arbitrarily converted selective gradients to numerical values: for continuous landscapes, we used the value of the continuous habitat (ranging between 0 and 1) occupied by each individual; for discrete landscapes, we used the value of the discrete habitat (0 or 1, corresponding to '*aa*' or '*AA*' habitat) occupied by each individual. Local adaptation was then determined by Pearson correlation between the allele frequency and selective gradient.

Genotype–environment association methods

We used both multivariate and univariate GEAs to assess the genetic signature of local adaptation. Multivariate ordination methods take two main forms: indirect ordinations, which use internal patterns of association in the genetic data to explain as much genetic variability as possible in the smallest number of axes; and constrained ordinations, which use a similar approach but restrict the ordination axes to be combinations of supplied explanatory variables. We used two indirect ordinations and two constrained ordinations to detect covariation between allele frequencies and environmental variables (described below). More details of ordination methods can be found in Legendre & Legendre (2012), with representative applications to genetic data in Jombart *et al.* (2009).

Principal components analysis (PCA) is an indirect ordination that constructs a new set of axes for a multivariate data set that maximally explain the variance in the data. This approach uses linear combinations of the original axes and preserves the Euclidean distance among objects. Principal coordinate analysis (PCoA) is an indirect ordination similar to PCA. However, PCoA is an eigenanalysis of the distance (or any distance-based metric) among observations. Where PCA uses linear combinations of the original axes, PCoA axes are influenced by the chosen distance metric, producing a representation of objects in Euclidean space while preserving the chosen distance metric. For example, PCoA of a Euclidean distance matrix would yield a PCA solution.

Redundancy analysis (RDA) is a constrained ordination that extends linear regression to multivariate response data in order to maximize the proportion of the response variable that is explained. Linear combinations of the response variable (in this case, genetic data) are modelled as a function of linear combinations of the predictors (in this case, environmental data). Redundancy analysis involves a two-step process in which a multivariate linear regression is computed between genetic and environmental data to produce a matrix of fitted values, and then a PCA of the fitted values produces canonical axes, which are linear combinations of the original explanatory variables. Distance-based redundancy analysis (dbRDA) is the constrained version of PCoA and the analogue of an RDA based on a dissimilarity matrix. In this case, genetic data are subject to PCoA and the resulting eigenvectors are used as the response variable in RDA, producing the dbRDA ordination.

We compared these ordination methods to latent factor mixed models (LFMMs), which use a hierarchical Bayesian mixed modelling approach to identify allele–environment correlations, while modelling residual population structure with 'latent factors' (Frichot *et al.* 2013). Latent factors are similar to principal components; in fact, when the number of latent factors (K) equals the number of loci in the data set, it is analogous to a PCA (Frichot *et al.* 2013). The computational efficiency of LFMMs comes from the flexibility to use a smaller latent factor value than the total number of loci. The value of K can have a large impact on LFMM results: larger values of K increase false-negative rates, while smaller values of K increase false-positive rates. For this reason, we used two approaches to determine the value of K (see below).

Genetic data were coded as the number of '*A*' alleles at each locus (monomorphic loci were removed). We standardized genetic and environmental data (i.e. scaled to unit standard deviation and centred on the mean) for PCA and RDA and calculated multivariate Bray–Curtis distances for PCoA and dbRDA. For continuous selection gradient analyses, we standardized two independent environmental variables: the *x*-coordinate location of an individual ('*x*') and the y-coordinate location of an individual ('*y*'). For discrete selection simulations, a third standardized habitat variable ('*habitat*') was also used, which describes whether an individual was located in an '*AA*' or '*aa*' patch (calculated using the 'RASTER' package, Hijmans 2014).

For all ordinations, outlier loci were identified on each of the first three ordination axes as those loci with a 'locus score' that was ±3 SD from the mean score for that axis. Locus scores are the coordinates of each locus in the ordination space (called 'species scores' in the 'VEGAN' package). For PCoA, where locus scores are not automatically calculated, we computed weighted average scores for each locus using the ordination score and SNP allele frequency (function '*wascores*' in 'VEGAN'). Once outlier loci were identified, they were then tested for association with environmental variables by calculating the correlation between the allele frequencies at that locus and each environmental variable. Significant relationships had a *P*-value <0.001. All ordinations were conducted using the 'VEGAN' package.

For LFMMs, we used two methods to determine the value of *K*: the Patterson method (also called the Tracy–Widom test, Patterson *et al.* 2006) and the minimum average partial test (MAP, Shriner 2012). While the Patterson approach tends to overestimate the number of significant principal components, resulting in larger values of *K*, the MAP approach tends to estimate smaller values of *K* (Table S3, Supporting information). Values of *K* were calculated using the 'RMTSTAT' package (Johnstone *et al.* 2009) and code provided by Daniel Shriner (2012). Results were comparable across both *K* selection methods; however, the Patterson approach generally resulted in lower false-positive rates. LFMM results using the Patterson *K* are presented here, with MAP *K* results presented in Table S4, Supporting information. We ran LFMMs using the command line version (1.2) for LINUX, downloaded from http://membres-timc.imag.fr/Eric.Frichot/lfmm/software.htm. We used 1200 iterations and a burn-in period of 200 and tested a subset of models to ensure results converged at this run length. LFMM outliers were detected as those loci with a *P*-value <0.001 after Bonferroni correction.

For each GEA method, we calculated the following metrics and averaged across 10 replicates for each simulation scenario: true-positive rate (TPR, the number of correct positive detections of one possible), false-positive rate (FPR, the number of incorrect positive detections of 99 possible) and a 'GEA index' that assesses parameter estimation for each method (i.e. correctly identifying the driving environmental variable). The GEA index ranges between 3 (best performance) and 0 (worst performance) and was coded as follows for continuous selection gradients, where the locus under selection was driven by *y*: 3 = the correct identification: *y* is the most significant variable identified; 2 = *y* is significant but less significant than *x*; 1 = *y* is not detected as significant, but *x* is detected; and 0 = no environmental variable is detected. Similarly, the GEA association index for discrete selection simulations was coded as follows: 3 = the correct identification: *habitat* is the most significant variable identified; 2 = *habitat* is significant but less so than *y* or *x*, 1 = *habitat* is not detected as significant, but *y* or *x* are detected; and 0 = no environmental variable is detected as significantly associated with the locus under selection. Spurious correlations (GEA index = 1) were distinguished from 'no detection' (GEA index = 0) because we expect that the spatial dependence of environmental predictors will sometimes result in correct identification of a locus under selection but incorrect detection of the driving predictor (Wagner & Fortin 2005).

Results

Isolation by distance and local adaptation

We assessed genomewide IBD using spatial eigenfunction analysis and RDA. As expected, dispersal distance primarily shaped patterns of IBD across simulations. IBD increased with decreasing dispersal distance, ranging from a minimum $R^2_{adj} = 0.01$ at 50% dispersal capacity to a maximum $R^2_{adj} = 0.36$ at 3% dispersal capacity (Fig. 2a). By contrast, increasing selection strength and increasing aggregation of habitat (i.e. factors that increase the strength of local adaptation) led to only small increases in patterns of genomewide IBD (Fig. 2a). Detection of IBD via spatial eigenfunction/RDA analysis and Mantel's tests were comparable, although the strength of the relationship was always weaker for Mantel's tests (Table S2, Supporting information; Diniz-Filho *et al.* 2013).

The strength of local adaptation was determined by quantifying the relationship between the allele frequency of the selected locus and selection gradients. Habitat configuration had a major effect on the strength of local adaptation. Overall, local adaptation increased with increasing levels of habitat aggregation (i.e. lowest for H1 and highest for continuous gradient habitats,

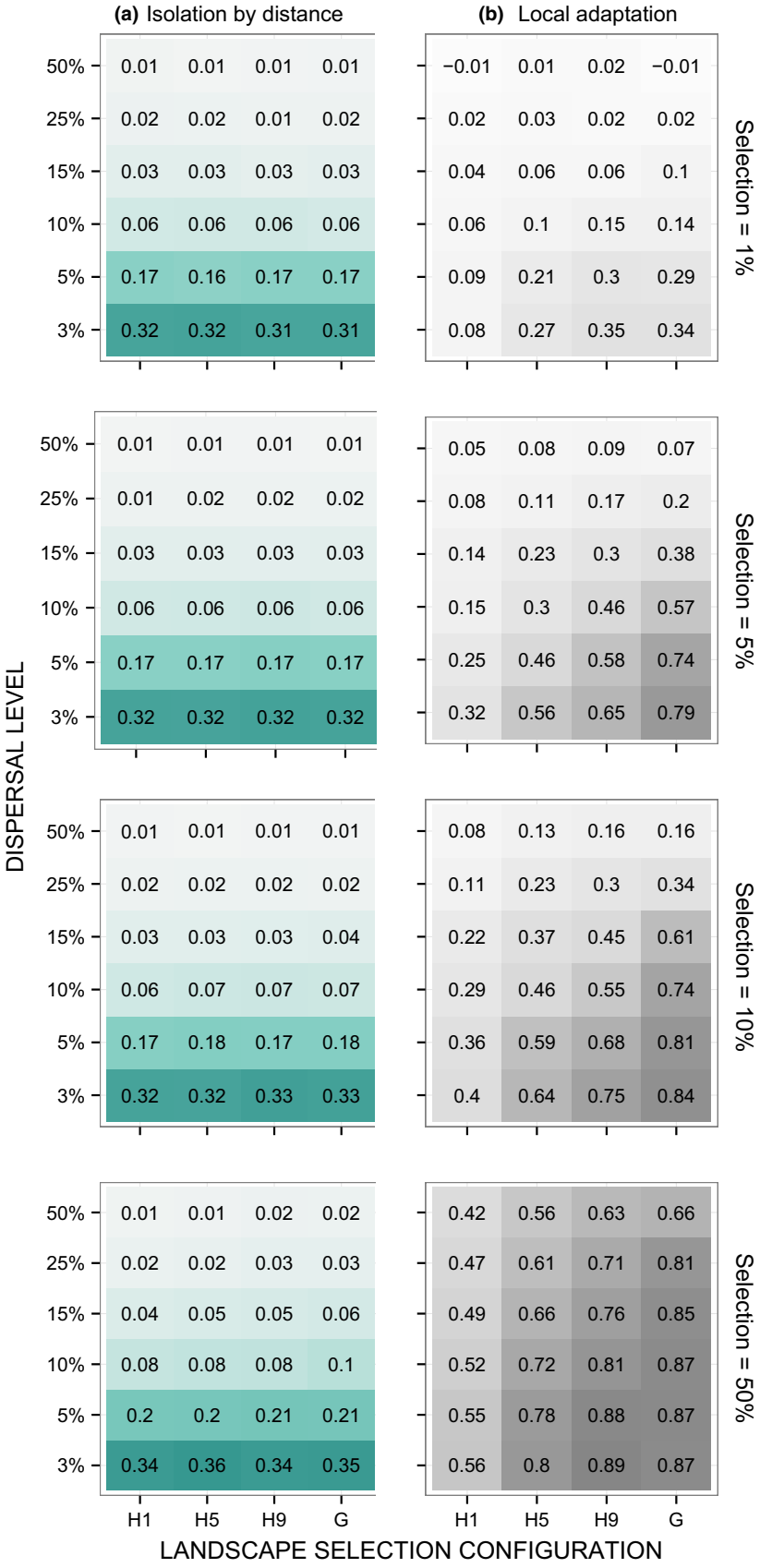

Fig. 2 Isolation by distance, assessed by spatial eigenfunction and redundancy analysis, averaged across ten replicates of each simulation scenario (a). The strength of local adaptation, assessed by correlation between the selected locus and environment, averaged across ten replicates of each simulation scenario (b).

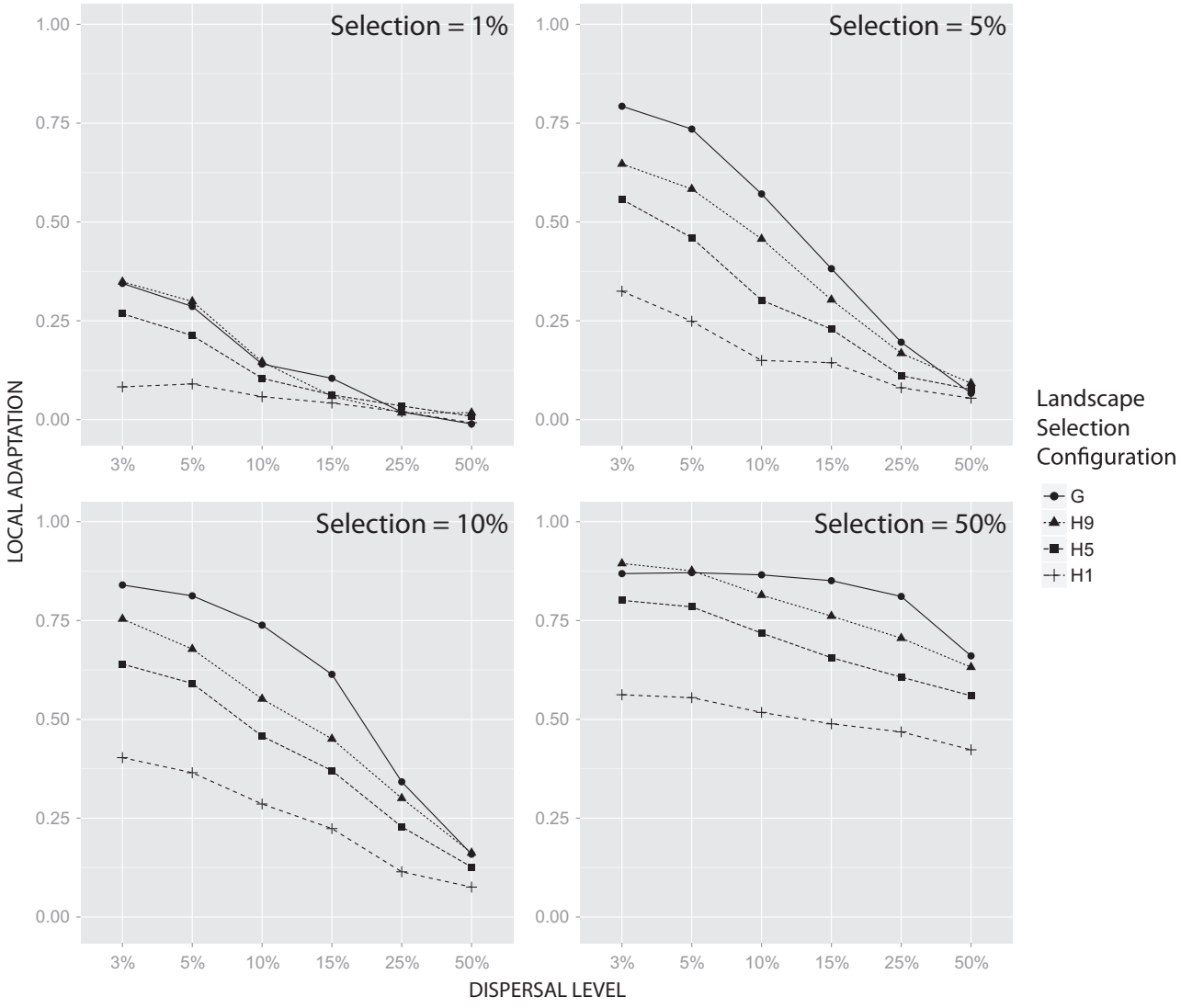

Fig. 3 Strength of local adaptation across dispersal levels and landscape selection configurations, with one plot per selection strength. Local adaptation is assessed by correlation between the selected locus and environment, averaged across ten replicates of each simulation scenario.

Figs 2b and 3). The effect of habitat configuration on the strength of local adaptation was weakest under high dispersal and weak selection and became stronger as dispersal decreased and selection increased (Fig. 3). All landscape configurations showed a pattern of larger increases in local adaptation from 1% to 5% selection and 10% to 50% selection, with a much smaller increase from 5% to 10% selection (Fig. 3).

Dispersal level had the strongest effect on patterns of local adaptation under moderate (5% and 10%) selection strengths (Fig. 3). The average increase in the strength of local adaptation from the highest (50%) to the lowest (3%) dispersal level was nearly two times greater under 5% and 10% selection compared to 1% and 50% selection (Fig. 3). At the highest dispersal levels (25–50%), the strength of local adaptation remained high under 50% selection (Fig. 3), indicating that selection was strong enough to maintain local adaptation despite high gene flow.

Effects of landscape, selection, and dispersal on detection probability

We found that highly aggregated selection landscapes (continuous selection gradients, highly aggregated discrete habitats) produced stronger local adaptation (Figs 2b and 3) and correspondingly detection methods were generally more powerful (higher TPRs, Fig. 4) and better able to detect the driving environmental variable (stronger GEA indices, Fig. 5).

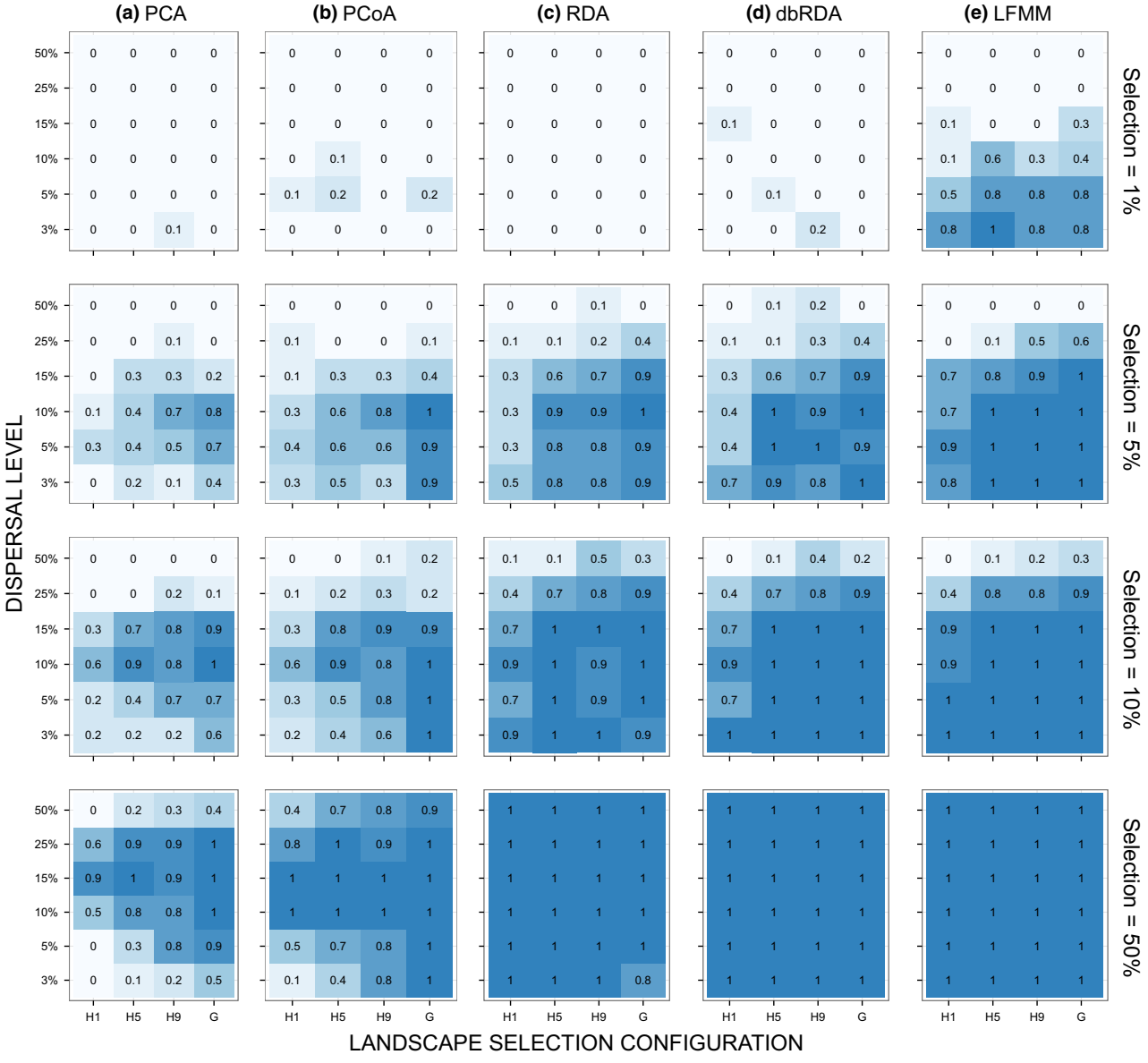

Fig. 4 Average true-positive rate (TPR) across ten replicates of each simulation scenario. TPR scales from 0 (worst performance, 0% TPR, light shades) to 1 (best performance, 100% TPR, dark shades). Results for (a) principal components analysis, (b) principal coordinate analysis, (c) redundancy analysis, (d) distance-based redundancy analysis and (e) latent factor mixed models.

Under 1% selection the selected locus was rarely detected by most methods, regardless of dispersal level (Fig. 4). Under 5% and 10% selection, TPRs were negatively associated with dispersal capacity, with the highest dispersal values inhibiting detection of the selected locus. However, with 50% selection, TPRs for most methods were high regardless of dispersal capacity. Generally, lower dispersal rates resulted in higher levels of IBD and local adaptation (Fig. 2), accompanied by higher TPRs (Fig. 4) and stronger GEA indices (Fig. 5).

Method comparison

False-positive rates across ordination methods were uniformly low (0–2%, Fig. 6a–d) and unaffected by habitat configuration, selection strength or dispersal capacity. The univariate method we tested, LFMM (using Patterson K), had much higher FPRs compared to ordination methods at low-to-moderate dispersal levels (3–15%). Average FPRs greater than 40% were common for LFMM with 3% and 5% dispersal, with a maximum average FPR of 55% on gradient selection

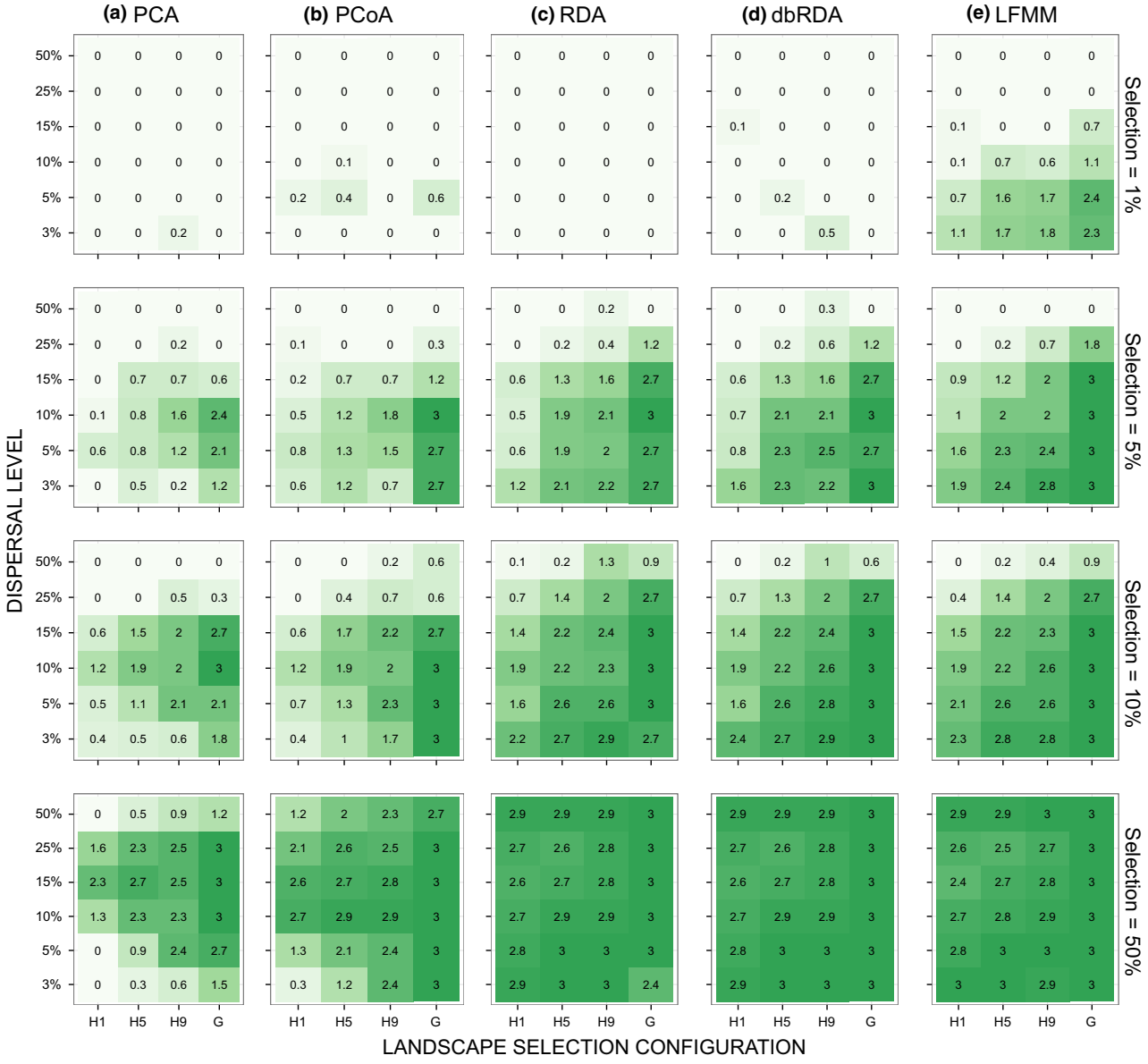

Fig. 5 Average genotype–environment association (GEA) index across ten replicates of each simulation scenario. Correct detection (3) has dark shading, with no detection (0) in light shading. Results for (a) principal components analysis, (b) principal coordinate analysis, (c) redundancy analysis, (d) distance-based redundancy analysis and (e) latent factor mixed models.

surfaces (Fig. 6e). Although LFMMs had the highest power under weak selection/low dispersal simulations (Fig. 4e), FPRs for these scenarios averaged 40% (Fig. 6e). Ordinations had uniformly low TPRs and FPRs across weak selection scenarios. FPRs for no selection simulations (used as a null model) were nearly identical to FPRs in selection simulations (Fig. S1, Supporting information).

Of the four ordination methods, constrained ordinations (RDA and dbRDA) had the highest TPRs (Fig. 4) and strongest GEA indices (Fig. 5) across all scenarios when compared to indirect methods (PCA and PCoA). TPRs and GEA indices were generally high across most dispersal levels for constrained ordinations, while indirect methods showed a pattern of stronger TPRs and GEA indices at intermediate dispersal levels.

Effect of mutation rate

A subset of the simulations were run with a zero mutation rate to assess the impact of the chosen mutation rate (0.0005 per generation) on detection results. Differences in detection rates, IBD and local adaptation were assessed with paired *t*-tests. There were few significant

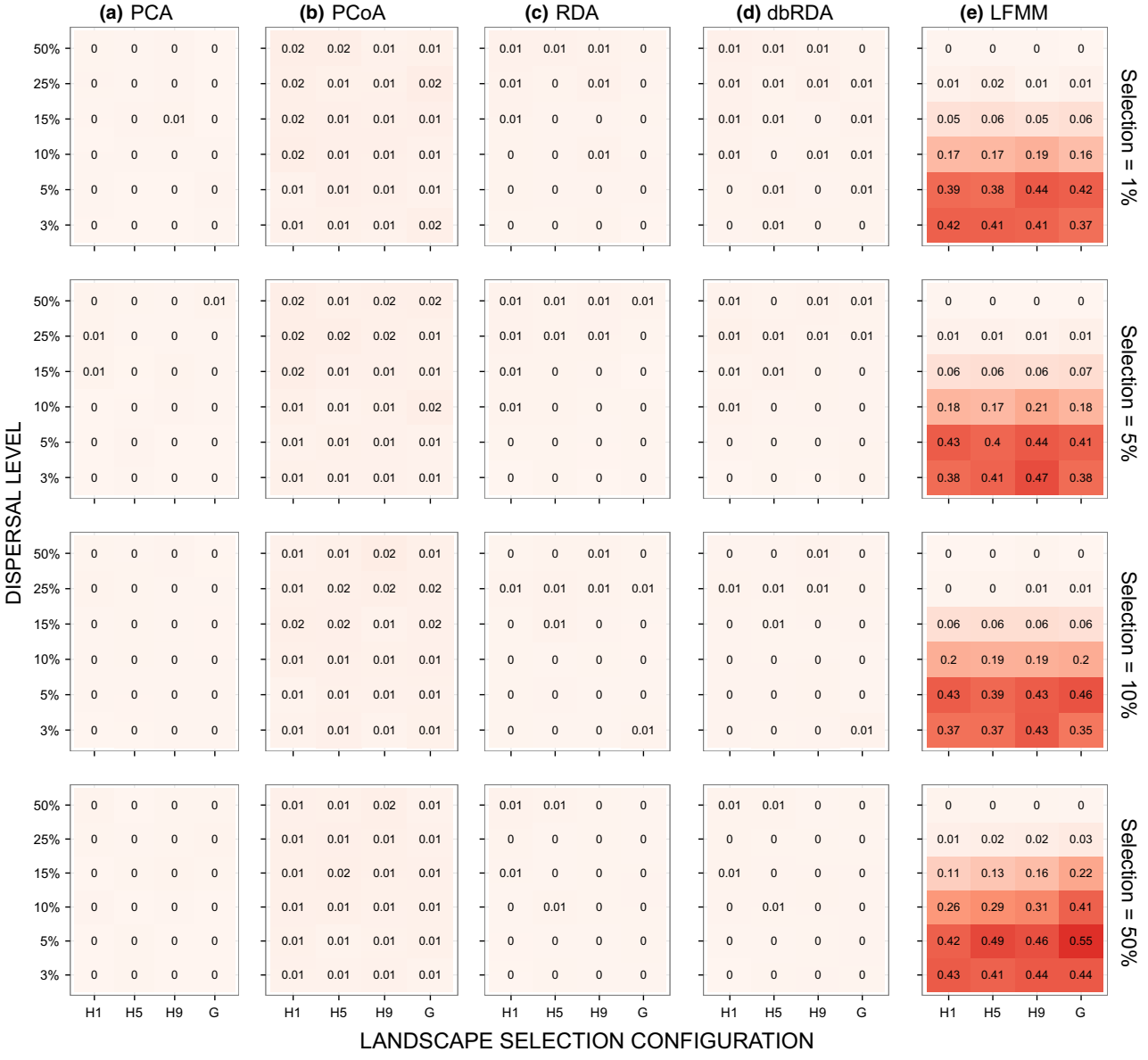

Fig. 6 Average false-positive rate (FPR) across ten replicates of each simulation scenario. FPR scales from 0 (best performance, 0% FPR, light shades) to 1 (worst performance, 100% FPR, dark shades). Results for (a) principal components analysis, (b) principal coordinate analysis, (c) redundancy analysis, (d) distance-based redundancy analysis and (e) latent factor mixed models.

differences at $\alpha = 0.05$: four cases for FPRs and two cases for IBD (Table S1, Supporting information).

Discussion

Spatial environmental variation plays a central role in maintaining spatial patterns of biodiversity, many of which are due to local adaptation. However, many populations fail to adapt along environmental gradients, partly due to the interaction between dispersal and the spatial structure of the environment. Existing knowledge of the relationship between spatial environmental structure and local adaptation has been largely based on the study of linear or monotonic environmental gradients (e.g. Holt & Gaines 1992; Kirkpatrick & Barton 1997), with few studies considering how the complexity of realistic landscapes may affect patterns of local adaptation (Holt & Barfield 2011; Schiffers *et al.* 2014). Our understanding of the geographic mosaic of selection depends on our ability to detect genomic signatures of selection in realistic landscapes. To this end, we examined how the interplay between environmental heterogeneity, dispersal ability and selection affects the strength of local adaptation and our ability to detect

selection in continuously distributed populations. Our study provides a quantitative assessment of the spatial, dispersal and selective conditions that favour the generation and maintenance of local adaptation, and may guide more accurate predictions regarding the strength of local adaptation in nature.

We found strong effects of habitat configuration on local adaptation, supporting previous work by Lotterhos & Whitlock (2014). The strength of local adaptation increased as habitat was more aggregated and as dispersal levels decreased (Figs 2b and 3). This pattern is a product of the interplay of habitat patchiness, and the chance a dispersing individual will end up in a suitable habitat patch (i.e. the flow of alleles across environmental gradients, Lenormand 2002). As habitat aggregation increases, the spatial autocorrelation in selective gradients also increases, decreasing the probability of gene flow between different selective regimes. Additionally, the effect of habitat configuration on local adaptation was greater under limited dispersal and stronger selection (Fig. 3). The lack of an effect of configuration under high dispersal and weak selection may be explained by the theoretical result of Slatkin (1973), who found that local adaptation will not occur below the 'characteristic length' (equal to the average dispersal distance divided by the square root of the selection differential). That is, when dispersal is high and selection weak, the characteristic length is very high, potentially higher than even our most aggregated landscapes. Indeed, in more spatially aggregated landscapes (H5, H9, and continuous gradient), weak selection was largely ineffective in generating a pattern of local adaptation, suggesting that when selection is weak the extent of landscape heterogeneity is of minor importance in shaping or preventing local adaptation. We did not find evidence that habitat aggregation mediated nonlinear effects of dispersal on local adaptation via effects on genetic variance (Barton 2001), likely because evolution in our simulations was not limited by genetic variance. Our findings closely parallel results from stochastic spatially explicit simulations of both population genetics (Behrman & Kirkpatrick 2011; Schiffers *et al.* 2014) and ecological communities (Palmer 1992; Lasky & Keitt 2013), where dispersal and the spatial structure of environmental gradients interact to determine the importance of the environment in driving spatial biodiversity.

We found that local adaptation in our simulated fine-grained landscapes (H1) occurred even in the face of substantial gene flow when selection was moderate to strong (10–50%, Figs 2b and 3). Our findings support results from empirical case studies of local adaptation to small, patchily distributed habitats, known as microgeographic adaptation (Allen & Sheppard 1971; Tack & Roslin 2010; Richardson *et al.* 2014), which requires very strong selective gradients or very restricted gene flow (Slatkin 1975). Additionally, the more pronounced decline in local adaptation with increasing gene flow for moderate selection strengths (5–10%) illustrates a shift in the migration–selection balance response across selection levels; while weak (1%) and strong (50%) selection show only modest changes in local adaptation across dispersal levels (very low and very high levels of local adaptation for 1% and 50% selection, respectively), moderate selection strengths are much more sensitive to increasing gene flow (Fig. 3).

We found evidence for modest genomic divergence driven by limitations on gene flow due to selection (i.e. 'isolation by environment', Barton 1979; Wang & Bradburd 2014). Specifically, changes in habitat aggregation and the strength of selection had small effects on spatial structure at neutral sites (Fig. 2a). The weak effect of selection on neutral sites here was likely due to the lack of physical linkage between loci in our simulations (i.e. high recombination) and monogenic local adaptation (Barton 1979).

We did not explore several factors that may play an important role in determining the strength of local adaptation and our ability to detect it, such as carrying capacity and genetic architecture. Carrying capacity can interact with dispersal to affect local adaptation, as lower carrying capacity increases the chance of population extinction under high migration load (Bridle *et al.* 2010). Additionally, polygenic architecture may interact with spatial structure of the environment. Schiffers *et al.* (2014) found that the effects of the spatial structure of selective gradients on local adaptation are contingent on the genetic architecture of traits under selection, such that under some scenarios, local adaptation is weaker for polygenic traits in highly aggregated habitats. In general, migration load may be higher for polygenic traits (Lenormand 2002), due to swamping of many alleles with small fitness effects. The loci underlying polygenic local adaptation will be considerably more challenging to detect statistically (Yeaman 2015).

Evaluation of detection methods

To leverage information contained in population genomic data sets, it is essential to develop statistical approaches capable of robustly detecting loci underlying local adaptation in complex landscapes. This is a major challenge because the factors that facilitate local adaptation (e.g. limited dispersal) may also produce genomewide patterns that confound the detection of loci under selection (e.g. population structure and IBD). As expected, detection methods generally had their poorest performance under combinations of weak (1%) selection, high dispersal (25–50%) and high habitat

heterogeneity (H1). Increasing selection from 1% to 5% resulted in pronounced overall improvement to detection rates, especially for ordination methods (Figs 4 and 5).

The most striking result from our methods comparison is the ability of ordination techniques to effectively control for population structure due to IBD, a major contributor to high false-positive rates when testing for loci under selection (Meirmans 2012). Ordination methods produced uniformly low FPRs (0–2%, Fig. 6a–d), in contrast to LFMMs, which produced very high FPRs (up to 55%, Fig. 6e) under low dispersal scenarios. Low dispersal generates high levels of IBD (Fig. 2a), contributing to spurious genotype–environment correlations (Meirmans 2012). However, under weak (1%) selection and limited dispersal, there is a trade-off between power to detect local adaptation and controlling for IBD. Ordinations have uniformly low power under weak selection, while LFMM have higher power under weak selection/low dispersal scenarios (Fig. 4), which comes at the cost of high false-positive rates (39–44%, Fig. 6e). While LFMMs incorporate latent factors in an effort to control for population structure, we find that this approach is insufficient for the strong signals of IBD generated with low dispersal. This is likely due to the ambiguity in determining the number of latent factors (*K*) at low dispersal levels in our individual-based framework (Table S3, Supporting information). In low dispersal simulations, there was large disagreement between the two assessments of *K* (the Patterson and MAP approaches), whereas in higher dispersal simulations, the two methods converged on a similar value (Table S3, Supporting information). The reasons for divergence in estimating *K* under high IBD scenarios are unclear. However, even when using the more conservative Patterson method to assign *K*, FPRs were high in cases of strong IBD (Figs. 6e and 2a).

Ordinations take a different approach to controlling for population structure that does not require the a priori assignment of structure. Generally, the ordinations tested here take the multidimensional scatter of genetic data and create a reduced set of axes that maximize the variability explained (Legendre & Legendre 2012). Because processes that produce population structure are expected to affect all neutral loci in a similar manner, these loci will tend not to show unique or unusual patterns in the ordination space; instead, the first few ordination axes will capture these main drivers of structure.

Among the four ordination methods, we found two interesting patterns: (i) constrained ordinations have the highest TPRs (Fig. 4) and strongest GEA indices (Fig. 5) across all scenarios when compared to indirect methods; and (ii) indirect methods show a pattern of stronger GEA indices and TPRs at intermediate dispersal levels. The better performance of constrained over indirect ordinations is related to differences in how the ordination axes are derived between the two approaches. Constrained ordinations find combinations of multiple predictor variables that explain multiple response variables. The inclusion of predictor variables that are thought to drive selection essentially reorders the ordination axes to prioritize trends explained by those variables. In the case of our simulations, this means that the locus under selection will tend to be detected on one of the first three constrained axes (since we used three explanatory variables, Fig. 7c,d). By contrast, indirect ordinations, which proceed based solely on internal patterns of variability in the genetic data (with no reference to environment), are unlikely to detect the locus under selection within the first few ordination axes. This is because the anomalous pattern created by that locus is unlikely to have a signal that is strong enough to load on the first few axes (Fig. 7a,b).

This difference in how the ordination axes are prioritized between indirect and constrained methods may also explain why the adaptive signals detected by indirect ordinations were strongest at intermediate dispersal levels (Figs 4a,b and 5a,b). When dispersal was very high, gene flow resulted in the selected locus being common in areas where it was maladaptive, weakening the signal of local adaptation (Fig. 2b, García-Ramos & Kirkpatrick 1997; Lenormand 2002; Garant *et al.* 2007). When dispersal was limited, the adaptive signal was relegated to minor axes (with low overall explanatory power) because the first few ordination axes were dominated by explaining the high IBD signal in the data (Fig. 2a, Fig. 7a,b). Searching through all of the minor axes (in this case 100 axes total) for the outlier signal would likely result in a very high false-positive rate.

These results make a strong case for constrained ordinations as an important GEA analytical tool due to their high power under moderate to strong selection combined with very low false-positive rates (0–1%). Additionally, these methods can reveal genetic structure varying from clusters to clines, have no underlying population genetic assumption (e.g. Hardy–Weinberg equilibrium) and are computationally efficient (Jombart *et al.* 2009). Their low power under weak (1%) selection, however, points to the utility of taking an ensemble detection approach, using multiple methods and looking for agreement across approaches (Jones *et al.* 2013). However, there is additional evidence from other simulation work (e.g. Tiffin & Ross-Ibarra 2014) that weak selection is difficult to detect no matter what methods are used; this will be an important area for further research (see below).

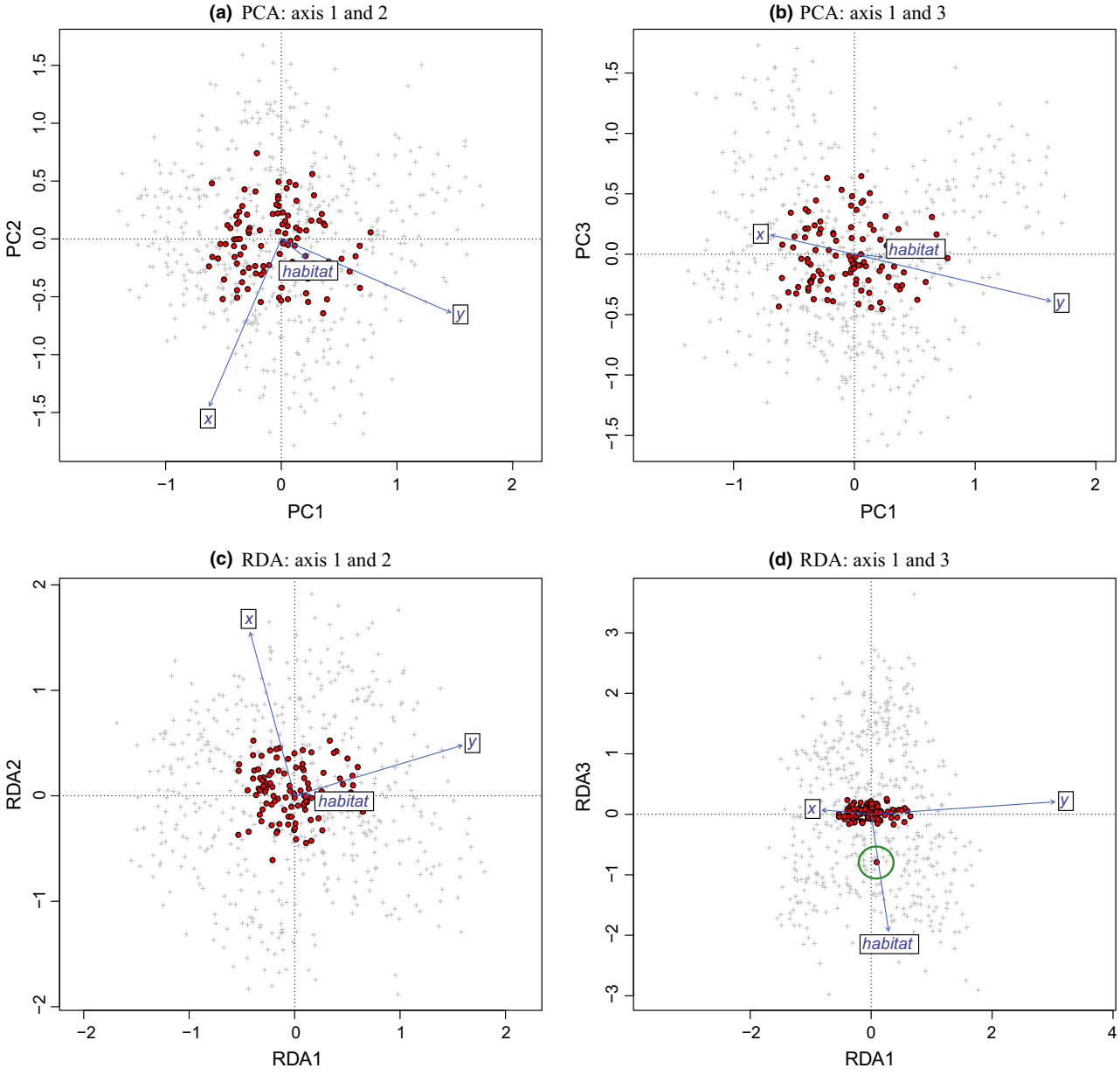

Fig. 7 Examples of ordination plots for PCA (top row) and RDA (bottom row). Simulation plotted is replicate 10 from the H1 landscape configuration, strong (50%) selection and 5% dispersal. Plots show the distribution of loci (red circles) and individual genotypes (grey pluses) in the ordination space. The correlation of the predictor variables with the axes is shown with the blue vectors. In this case, PCA did not detect the selected locus on the first three axes (a-b), while RDA did detect the selected locus (circled in green) on axis 3, correctly correlated with *habitat* (d). Note how *x* and *y* load strongly on the first two RDA axes (c), while *habitat* loads strongly on RDA axis 3 (d). This is in contrast to PCA, where *habitat* fails to load strongly on any of the first three axes (a, b).

Future directions

The number of simulation parameters we tested was necessarily limited to examine how combinations of habitat aggregation, dispersal capacity and selection strength affected local adaptation and detection performance. Many variables remain to be tested including the effects of conditional neutrality (Tiffin & Ross-Ibarra 2014), temporally fluctuating selection, new mutation vs. standing variation, trait dominance, complex demographic scenarios (e.g. population expansions along environmental gradients), population size, and sampling scheme (following up on work by Lotterhos & Whitlock 2015). The ability of GEA methods to detect multilocus selection in a controlled framework also remains untested. This is an important element for future research because adaptation often occurs via

coordinated shifts in allele frequencies across large numbers of loci, many of small effect (Imhof & Schlötterer 2001; Kassen & Bataillon 2006; Le Corre & Kremer 2012; Harrisson *et al.* 2014; Yeaman 2015). A recent empirical investigation showed the promise of multivariate methods for detecting these polygenic signals of local adaptation (Bourret *et al.* 2014), while other studies suggest detecting these loci may be inherently challenging (Yeaman 2015). Studies that address the above issues will further our understanding of the conditions that shape local adaptation in wild populations and how our ability to detect selection changes under these conditions.

Acknowledgements

We would like to thank Dean L. Urban for helpful comments and discussion, and three anonymous reviewers and the editor for valuable feedback on earlier versions of the manuscript. BRF is supported by a Katherine Goodman Stern Fellowship provided by the Duke University Graduate School. MRJ is supported by a National Science Foundation Graduate Research Fellowship under Grant No. DGE-1313190. Computational resources for simulation and analysis were provided by the University of Montana Computational Ecology Laboratory. This work resulted from a Distributed Graduate Seminar in Landscape Genetics supported by the Canadian Institute of Ecology and Evolution (CIEE) and the American Genetics Association (AGA).

References

Allen WR, Sheppard PM (1971) Copper tolerance in some Californian populations of the monkey flower, *Mimulus guttatus*. *Proceedings of the Royal Society of London. Series B, Biological Sciences*, **177**, 177–196.

Austin MP (1987) Models for the analysis of species' response to environmental gradients. *Vegetatio*, **69**, 35–45.

Balloux F (2001) EASYPOP (Version 1.7): a computer program for population genetics simulations. *Journal of Heredity*, **92**, 301–302.

Barton NH (1979) Gene flow past a cline. *Heredity*, **43**, 333–339.

Barton NH (2001) Adaptation at the edge of a species' range. In: *Integrating Ecology and Evolution in a Spatial Context* (eds Silvertown J, Antonovics J), pp. 365–392. Blackwell Science Ltd, Oxford, UK.

Behrman KD, Kirkpatrick M (2011) Species range expansion by beneficial mutations. *Journal of Evolutionary Biology*, **24**, 665–675.

Bell G, Gonzalez A (2011) Adaptation and evolutionary rescue in metapopulations experiencing environmental deterioration. *Science*, **332**, 1327–1330.

Blanchet FG, Legendre P, Borcard D (2008) Forward selection of explanatory variables. *Ecology*, **89**, 2623–2632.

Bourret V, Dionne M, Bernatchez L (2014) Detecting genotypic changes associated with selective mortality at sea in Atlantic salmon: polygenic multilocus analysis surpasses genome scan. *Molecular Ecology*, **23**, 4444–4457.

ter Braak CJF (1987) The analysis of vegetation-environment relationships by canonical correspondence analysis. In: *Theory and Models in Vegetation Science* (eds Prentice IC, van der Maarel E), pp. 69–77. Springer, Netherlands.

Bray JR, Curtis JT (1957) An ordination of the upland forest communities of southern Wisconsin. *Ecological Monographs*, **27**, 325–349.

Bridle JR, Polechová J, Kawata M, Butlin RK (2010) Why is adaptation prevented at ecological margins? New insights from individual-based simulations. *Ecology Letters*, **13**, 485–494.

Canty A, Ripley B (2012) *boot: Bootstrap R (S-Plus) functions*. R package version 1.3-5.

Cavalli-Sforza LL (1966) Population structure and human evolution. *Proceedings of the Royal Society of London. Series B, Biological Sciences*, **164**, 362–379.

Coop G, Witonsky D, Rienzo AD, Pritchard JK (2010) Using environmental correlations to identify loci underlying local adaptation. *Genetics*, **185**, 1411–1423.

De Mita S, Thuillet A-C, Gay L *et al.* (2013) Detecting selection along environmental gradients: analysis of eight methods and their effectiveness for outbreeding and selfing populations. *Molecular Ecology*, **22**, 1383–1399.

De Villemereuil P, Frichot É, Bazin É, François O, Gaggiotti OE (2014) Genome scan methods against more complex models: when and how much should we trust them? *Molecular Ecology*, **23**, 2006–2019.

Diniz-Filho JAF, Soares TN, Lima JS *et al.* (2013) Mantel test in population genetics. *Genetics and Molecular Biology*, **36**, 475–485.

Dray S, Legendre P, Blanchet G (2011) *packfor: Forward selection with permutation (Canoco p.46)*. R package version 0.0-8/r100.

Duforet-Frebourg N, Laval G, Bazin E, Blum MGB (2015) Detecting genomic signatures of natural selection with principal component analysis: application to the 1000 Genomes data. arXiv:1504.04543v5 [q-bio.PE]

Endler JA (1973) Gene flow and population differentiation studies of clines suggest that differentiation along environmental gradients may be independent of gene flow. *Science*, **179**, 243–250.

Felsenstein J (1976) The theoretical population genetics of variable selection and migration. *Annual Review of Genetics*, **10**, 253–280.

Felsenstein J (1977) Multivariate normal genetic models with a finite number of loci. In: *Proceedings of the International Conference on Quantitative Genetics* (eds Pollak E, Kempthorne O, Bailey TB Jr), pp. 227–245. Iowa State University Press, Iowa, USA.

Fitzpatrick MC, Keller SR (2015) Ecological genomics meets community-level modelling of biodiversity: mapping the genomic landscape of current and future environmental adaptation. *Ecology Letters*, **18**, 1–16.

Frean M, Rainey PB, Traulsen A (2013) The effect of population structure on the rate of evolution. *Proceedings of the Royal Society B: Biological Sciences*, **280**, 1–7.

Frichot E, Schoville SD, Bouchard G, François O (2013) Testing for associations between loci and environmental gradients using latent factor mixed models. *Molecular Biology and Evolution*, **30**, 1687–1699.

Galinsky KJ, Bhatia G, Loh P-R *et al.* (2015) Fast principal components analysis reveals convergent evolution of ADH1B gene in Europe and East Asia. *bioRxiv*. doi: 10.1101/018143.

Garant D, Forde SE, Hendry AP (2007) The multifarious effects of dispersal and gene flow on contemporary adaptation. *Functional Ecology*, **21**, 434–443.

García-Ramos G, Kirkpatrick M (1997) Genetic models of adaptation and gene flow in peripheral populations. *Evolution*, **51**, 21–28.

Gardner RH (1999) RULE: map generation and a spatial analysis program. In: *Landscape Ecological Analysis* (eds Klopatek JM, Gardner RH), pp. 280–303. Springer, New York, USA.

Goslee S, Urban D (2007) The ecodist package for dissimilarity-based analysis of ecological data. *Journal of Statistical Software*, **22**, 1–19.

Günther T, Coop G (2013) Robust identification of local adaptation from allele frequencies. *Genetics*, **195**, 205–220.

Hahn MW (2008) Toward a selection theory of molecular evolution. *Evolution*, **62**, 255–265.

Haldane JBS (1930) A mathematical theory of natural and artificial selection (Part VI, Isolation). *Mathematical Proceedings of the Cambridge Philosophical Society*, **26**, 220–230.

Harrisson KA, Pavlova A, Telonis-Scott M, Sunnucks P (2014) Using genomics to characterize evolutionary potential for conservation of wild populations. *Evolutionary Applications*, **7**, 1008–1025.

Hedrick PW (1986) Genetic polymorphism in heterogeneous environments: a decade later. *Annual Review of Ecology and Systematics*, **17**, 535–566.

Hedrick PW (2006) Genetic polymorphism in heterogeneous environments: the age of genomics. *Annual Review of Ecology, Evolution, and Systematics*, **37**, 67–93.

Hedrick PW, Ginevan ME, Ewing EP (1976) Genetic polymorphism in heterogeneous environments. *Annual Review of Ecology and Systematics*, **7**, 1–32.

Hijmans RJ (2014) *raster: Geographic data analysis and modeling*. R package version 2.2-31.

Holt RD, Barfield M (2011) Theoretical perspectives on the statics and dynamics of species' borders in patchy environments. *The American Naturalist*, **178**, S6–S25.

Holt RD, Gaines MS (1992) Analysis of adaptation in heterogeneous landscapes: Implications for the evolution of fundamental niches. *Evolutionary Ecology*, **6**, 433–447.

Imhof M, Schlötterer C (2001) Fitness effects of advantageous mutations in evolving *Escherichia coli* populations. *Proceedings of the National Academy of Sciences USA*, **98**, 1113–1117.

Jensen JD, Kim Y, DuMont VB, Aquadro CF, Bustamante CD (2005) Distinguishing between selective sweeps and demography using DNA polymorphism data. *Genetics*, **170**, 1401–1410.

Johnstone IM, Perry PO, Ma Z, Shahram M (2009) *RMT: distributions, statistics and tests derived from random matrix theory*. R package version 0.2.

Jombart T, Pontier D, Dufour A-B (2009) Genetic markers in the playground of multivariate analysis. *Heredity*, **102**, 330–341.

Jones MR, Forester BR, Teufel AI *et al.* (2013) Integrating landscape genomics and spatially explicit approaches to detect loci under selection in clinal populations. *Evolution*, **67**, 3455–3468.

Joost S, Bonin A, Bruford MW *et al.* (2007) A spatial analysis method (SAM) to detect candidate loci for selection: towards a landscape genomics approach to adaptation. *Molecular Ecology*, **16**, 3955–3969.

Joost S, Vuilleumier S, Jensen JD *et al.* (2013) Uncovering the genetic basis of adaptive change: on the intersection of landscape genomics and theoretical population genetics. *Molecular Ecology*, **22**, 3659–3665.

Kassen R, Bataillon T (2006) Distribution of fitness effects among beneficial mutations before selection in experimental populations of bacteria. *Nature Genetics*, **38**, 484–488.

Kawecki TJ, Ebert D (2004) Conceptual issues in local adaptation. *Ecology Letters*, **7**, 1225–1241.

Kirkpatrick M, Barton NH (1997) Evolution of a species' range. *The American Naturalist*, **150**, 1–23.

Landguth EL, Cushman SA (2010) cdpop: a spatially explicit cost distance population genetics program. *Molecular Ecology Resources*, **10**, 156–161.

Lasky JR, Keitt TH (2013) Reserve size and fragmentation alter community assembly, diversity, and dynamics. *The American Naturalist*, **182**, E142–E160.

Lasky JR, Des Marais DL, McKay JK *et al.* (2012) Characterizing genomic variation of *Arabidopsis thaliana*: the roles of geography and climate. *Molecular Ecology*, **21**, 5512–5529.

Le Corre V, Kremer A (2012) The genetic differentiation at quantitative trait loci under local adaptation. *Molecular Ecology*, **21**, 1548–1566.

Legendre P, Legendre L (2012) *Numerical Ecology*. Elsevier, Amsterdam, The Netherlands.

Legendre P, Borcad D, Blanchet FG, Dray S (2012) *PCNM: MEM spatial eigenfunction and principal coordinate analyses*. R package version 2.1-2/r106.

Legendre P, Fortin M-J, Borcard D (2015) Should the Mantel test be used in spatial analysis? *Methods in Ecology and Evolution*, **6**, 1239–1247.

Lenormand T (2002) Gene flow and the limits to natural selection. *Trends in Ecology & Evolution*, **17**, 183–189.

Lotterhos KE, Whitlock MC (2014) Evaluation of demographic history and neutral parameterization on the performance of F_{ST} outlier tests. *Molecular Ecology*, **23**, 2178–2192.

Lotterhos KE, Whitlock MC (2015) The relative power of genome scans to detect local adaptation depends on sampling design and statistical method. *Molecular Ecology*, **24**, 1031–1046.

Mayr E (1963) *Animal Species and Evolution*. Harvard University Press, Cambridge, MA, USA.

Meirmans PG (2012) The trouble with isolation by distance. *Molecular Ecology*, **21**, 2839–2846.

Mitton JB, Linhart YB, Hamrick JL, Beckman JS (1977) Observations on the genetic structure and mating system of Ponderosa Pine in the Colorado front range. *Theoretical and Applied Genetics*, **51**, 5–13.

Mouquet N, Loreau M (2003) Community patterns in source-sink metacommunities. *The American Naturalist*, **162**, 544–557.

Nagylaki T (1975) Conditions for the existence of clines. *Genetics*, **80**, 595–615.

Oksanen J, Blanchet FG, Kindt R *et al.* (2013) *vegan: community ecology package*. R package version 2.0-10.

Orsini L, Spanier KI, De Meester L (2012) Genomic signature of natural and anthropogenic stress in wild populations of the waterflea *Daphnia magna*: validation in space, time and experimental evolution. *Molecular Ecology*, **21**, 2160–2175.

Paccard A, Vance M, Willi Y (2013) Weak impact of fine-scale landscape heterogeneity on evolutionary potential in *Arabidopsis lyrata*. *Journal of Evolutionary Biology*, **26**, 2331–2340.

Palmer MW (1992) The coexistence of species in fractal landscapes. *The American Naturalist*, **139**, 375–397.
Patterson N, Price AL, Reich D (2006) Population structure and eigenanalysis. *PLoS Genetics*, **2**, e190.
Price AL, Patterson NJ, Plenge RM *et al.* (2006) Principal components analysis corrects for stratification in genome-wide association studies. *Nature Genetics*, **38**, 904–909.
R Development Core Team (2012) *R: A Language and Environment for Statistical Computing*. R Foundation for Statistical Computing, Vienna, Austria.
Rellstab C, Gugerli F, Eckert AJ, Hancock AM, Holderegger R (2015) A practical guide to environmental association analysis in landscape genomics. *Molecular Ecology*, **24**, 4348–4370.
Richardson JL, Urban MC, Bolnick DI, Skelly DK (2014) Microgeographic adaptation and the spatial scale of evolution. *Trends in Ecology & Evolution*, **29**, 165–176.
Schiffers K, Schurr FM, Travis JMJ *et al.* (2014) Landscape structure and genetic architecture jointly impact rates of niche evolution. *Ecography*, **37**, 1218–1229.
Shriner D (2012) Improved eigenanalysis of discrete subpopulations and admixture using the minimum average partial test. *Human Heredity*, **73**, 73–83.
Slatkin M (1973) Gene flow and selection in a cline. *Genetics*, **75**, 733–756.
Slatkin M (1975) Gene flow and selection in a two-locus system. *Genetics*, **81**, 787–802.
Tack AJM, Roslin T (2010) Overrun by the neighbors: landscape context affects strength and sign of local adaptation. *Ecology*, **91**, 2253–2260.
Tiffin P, Ross-Ibarra J (2014) Advances and limits of using population genetics to understand local adaptation. *Trends in Ecology & Evolution*, **29**, 673–680.
Van den Wollenberg AL (1977) Redundancy analysis an alternative for canonical correlation analysis. *Psychometrika*, **42**, 207–219.
Wagner HH, Fortin MJ (2005) Spatial analysis of landscapes: concepts and statistics. *Ecology*, **86**, 1975–1987.
Wang IJ, Bradburd GS (2014) Isolation by environment. *Molecular Ecology*, **23**, 5649–5662.
Whittaker RH (1967) Gradient analysis of vegetation. *Biological Reviews*, **42**, 207–264.
Yeaman S (2015) Local adaptation by alleles of small effect. *The American Naturalist*, **186**, 1–16.
Yeaman S, Whitlock MC (2011) The genetic architecture of adaptation under migration–selection balance. *Evolution*, **65**, 1897–1911.

B.R.F., M.R.J., E.L.L. and J.R.L. designed the research. E.L.L. and B.R.F. ran the simulations. B.R.F. and J.R.L. performed the analyses. All authors interpreted the data and wrote the manuscript.

Data accessibility

Simulation data, landscape surfaces and individual sample files: Dryad doi:10.5061/dryad.v0c77. CDPOP software and user manual are available at: http://cel.dbs.umt.edu/cms/CDPOP.

Supporting information

Additional supporting information may be found in the online version of this article.

Table S1 Average true positive rates, false positive rates, and genotype-environment association indices across ten replicates of each simulation scenario for no mutation and mutation runs.

Table S2 Comparison of isolation by distance measures: simple Mantel's tests (Mantel r^2) and spatial eigenfunction and redundancy analysis (MEM-RDA R^2_{adj}); both metrics are averaged across ten replicates of each simulation scenario.

Table S3 The average value of K (the number of latent factors) across ten simulation replicates determined using the Minimum Average Partial Test (MAP) and Patterson approaches.

Table S4 Average true positive rate (TPR), false positive rate (FPR), and genotype-environment associations (GEA) across ten replicates of each simulation scenario for latent factor mixed models (LFMM) using the Minimum Average Partial Test (MAP) and Patterson K approaches.

Fig. S1 Average false positive rate (FPR) across ten replicates of 'no selection' simulations.